

Matrix-Isolation FT-IR Studies and *ab Initio* Calculations of Hydrogen-Bonded Complexes of Molecules Modeling Cytosine or Isocytosine Tautomers. 5. 1-CH₃-Cytosine Complexes with H₂O in Ar Matrices

Johan Smets,^{†,‡} Ludwik Adamowicz,^{§,||} and Guido Maes*,^{†,⊥}

Department of Chemistry, University of Leuven, Celestijnenlaan 200F, B-3001, Heverlee, Belgium,

Department of Chemistry, University of Arizona, Tucson, Arizona 85721, and Laboratoire de Physique Quantique, IR SAMC, Université Paul Sabatier, 118 Route de Narbonne, 31062 Toulouse Cedex, France

Received: April 25, 1995; In Final Form: January 2, 1996[⊗]

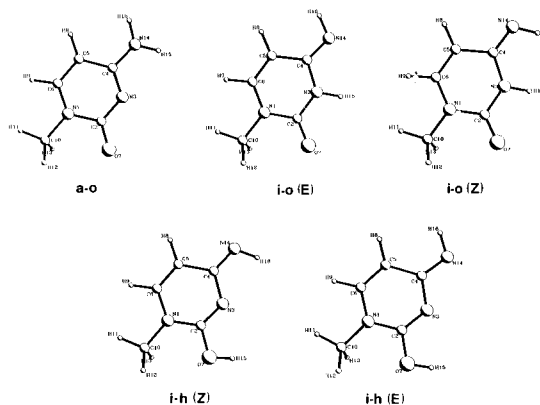
The combined experimental and theoretical *ab initio* method for investigation of hydrogen-bonded complexes between water and molecules modeling cytosines has been applied to 1-CH₃-cytosine. This compound occurs in Ar predominantly in the amino–oxo form, but traces of the imino–oxo *E* tautomer are also present in accordance with the *ab initio* prediction. An approximate value of 7.2 is obtained for the tautomerization constant $K_T(a-o/i-o)$ using the infrared intensity measurement. The most stable H-bonded complex of the abundant *a-o* tautomer with water is the closed N₃⋯H–O⋯H–N₁₄ structure, which shows cooperativity between the two H-bonds. Less stable complexes are the closed N₃⋯H–O–H⋯O₇ complex and the open N₁₄–H⋯OH₂ and N₁₄⋯H–OH structures. In the experimental FT-IR spectra, the closed N₃⋯H–O⋯H–N₁₄ and open O₇⋯H–OH complexes are identified based on characteristic absorptions predicted by *ab initio* calculations or based on earlier obtained experimental results for similar structures. Despite some trace amounts of the *i-o* *E* tautomer in the Ar matrix, H-bonding of this rare form with water was detected in the form of the closed N₁₄⋯H–O⋯H–N₃ structure. A preliminary correlation between the frequency shifts of the bonded water stretching mode and the proton affinities of the C=O group is presented for the open C=O⋯H–OH complexes of 1-CH₃-cytosine and some related compounds.

Introduction

In previous papers of this series we have reported results for tautomeric and H-bond properties of some molecules modeling cytosine or isocytosine.^{1–4} These results have been obtained by the combined experimental matrix-isolation FT-IR and theoretical *ab initio* method. In this paper we describe similar results for the tautomerism of 1-CH₃-cytosine (IMC) and its 1:1 H-bonded complexes with water in an inert Ar matrix environment.

From the biological point of view, IMC is the most important cytosine derivative, since it is an analogue of the nucleoside cytidine. Similar to the sugar ribose group in the latter compound, the methyl group attached to the N₁ atom blocks the oxo–hydroxy prototropism between the N₁ and O₇ sites. The amino–hydroxy (*a-h*) tautomer of cytosine has been demonstrated to be the most abundant form in inert Ar and N₂ matrices. Apart from a less abundant amino–oxo (*a-o*) form, a small amount of the rare imino–oxo (*i-o*) form of cytosine has also been observed in Ar.^{5–7} If the latter tautomer were present in cytidine during DNA or RNA polymerization, this could have rather important consequences for the fidelity of replication of the genetic material. The imino–oxo tautomer can form a stable base-pair with adenine, and this would lead to a point mutation.⁸ Fazakerly et al. have recently demonstrated that different tautomeric forms and base-pair configurations can be present simultaneously within a DNA base-pair.⁹ The

CHART 1



occurrence of the rare imino–oxo tautomer of IMC in an Ar matrix and in the gas phase was proven by Szczesniak et al. in 1992 with the use of UV experiments.¹⁰ Furthermore, two distinct rotamers *Z* and *E* around the double C₄N₈ bond were observed by those authors. Although a number of papers have reported semiempirical as well as *ab initio* calculations on the stability of the cytosine tautomers, most of them have been focused on unsubstituted cytosine. Also, in previously reported theoretical calculations on H-bond interaction of cytosines with water, only unsubstituted cytosines have been considered.^{11–15}

In this work we have calculated the stability of the three IMC tautomers amino–oxo (*a-o*), imino–oxo (*i-o*), and imino–hydroxy (*i-h*) as well as two rotamers of the imino forms (Chart 1). The results are compared to experimental data obtained for the base isolated in Ar. In the subsequent step, 1:1 H-bonded complexes of the two most stable forms of IMC with water have been considered. The *ab initio* predicted energy differences are compared to the relative concentrations of these complexes in the Ar matrix. Finally, a detailed comparison of

* Corresponding author.

[†] University of Leuven.

[‡] University of Arizona.

[§] Université Paul Sabatier.

^{||} Permanent address: Department of Chemistry, University of Arizona, Tucson, AZ 85721.

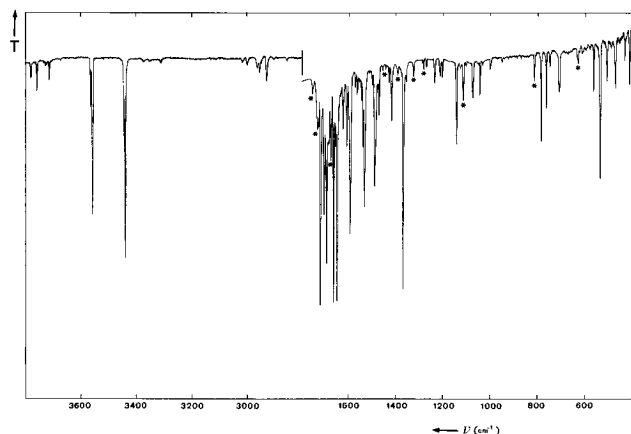
[⊥] Senior Research Associate of the Belgian National Fund for Scientific Research.

[⊗] Abstract published in *Advance ACS Abstracts*, March 15, 1996.

TABLE 1: Total (au) and Relative (kJ/mol) Energies and Dipole Moments (D) of the Amino–Oxo, Imino–Oxo, and Imino–Hydroxy Tautomers of 1MC Calculated at the MP2 Level with the 6-31++G Basis Set;^d Comparison to Literature Results**

method	amino–oxo	imino–oxo <i>E</i>	imino–oxo <i>Z</i>	imino–hydroxy <i>E</i>	imino–hydroxy <i>Z</i>
SCF	–431.675 045 0	–431.672 891 6	–431.669 887 6	–431.637 600 1	–431.644 190 3
MP2 ^a	–433.013 740 5	–433.009 564 7	–433.006 668 8	–432.977 818 8	–432.983 580 1
ZPE ^b	0.121 962 4	0.122 990 6	0.122 779 1	0.122 800 0	0.122 873 0
Total	–432.891 778 1	–432.886 574 1	–432.883 889 7	–432.855 020 0	–432.860 707 1
ΔE_T^c	0.00	13.69	20.72	96.74	81.63
μ (D)	6.97	5.55	3.11	6.60	5.99
AM1 ¹⁹	0.0	6.2			68.9
SCF/6-31G* ¹⁰	0.0	4.2	11.6		
SCF/6-31++G** (this work)	0.0	8.4	15.7	100.5	83.4
pseudopotential ²⁰	0.0	8.4			

^a Only valence correlation is considered. ^b Calculated as $0.9 \sum h\nu_i/2$. ^c Energy difference between tautomers. ^d Geometries optimized at the SCF/6-31++G** level.

**Figure 1.** FT-IR spectrum of 1-CH₃-cytosine in Ar at 12 K (* = imino–oxo *E* absorption).

the calculated and observed IR frequencies is made for the experimentally identified 1MC tautomers and its H-bonded complexes with water.

Methodology

Experimental. A detailed description of the cryogenic and FT-IR spectroscopic equipment has been given elsewhere.^{1,16,17} The optimal sublimation temperature for 1MC in Ar was 75 °C at the matrix deposition rate of about 5 mmol h^{–1}. Similar to all our earlier studies on water complexes in Ar, the varying water-to-base ratio from 1:1 to 1:5 was used. The latter ratio ensures that an excess amount of 1:1 complex species is present in the matrix with still weak spectral manifestations of higher stoichiometry complexes¹. 1MC was obtained from Sigma and was used without further purification.

Theoretical. The optimized geometries of the tautomers of the free base were determined at the SCF/6-31++G** level of theory. IR frequencies and intensities were also computed at this level with the use of the analytical derivative procedure incorporated in the Gaussian 92 program.¹⁸ Following these calculations, the total energies of the tautomeric forms were calculated at the MP2+0.9ZPE level (second-order Möller–Plesset perturbation theory for the electronic energy and scaled zero-point vibrational energy calculated with the use of the harmonic approximation with the SCF force constants obtained) using the same basis set. The calculated wavenumbers were scaled down by the uniform scaling factor of 0.90 to approximately correct for vibrational anharmonicity as well as for overestimation of the force constants at the SCF level. The same procedure has also been applied to the H-bonded complexes of 1MC with water. For the modes of bonded water, instead of using a uniform scaling factor, a varying, “optimal” scaling factor was applied.¹ The calculated interaction energies

for the complexes were corrected for the basis set superposition error (BSSE) by recalculating the monomer energies in the basis sets of the heterodimers. Detailed arguments for the use of all above procedures were described in the earlier reports of the series.^{1,2} In the complex involving the a–o form of 1MC there are two possible positions of the water molecule with one of the H atoms H-bonded to the N₃ ring atom. In the first position the water molecule forms a second H-bond with the 1MC NH₂ group, and in the second the second H-bond of water attaches to the carbonyl O atom. We should mention here that the theoretical calculation at the SCF/6-31++G** level does not predict the second structure to be a local minimum. At the SCF/6-31G** level, however, a stable structure was found for the N₃···H–O–H···O₇ complex. Although one can expect that this structure with both H atoms of water engaged in hydrogen bonds will be less stable than the structure with only one H atom and the O atom of water H-bonded, the SCF/6-31++G** result is somewhat unexpected. In order to verify this result, and in view of our earlier result that variation of the theoretical method may result in a slightly different geometry of the stable H-bonded structure in cases where in a closed complex two H-bonds B···H–O are present,⁴ MP2/6-31++G** geometry optimizations were carried out on the two water–1MC complexes. In this calculation a complex-stabilizing contribution not present in the SCF calculation is accounted for—the dispersion interaction. The MP2 optimizations resulted in only the N₃···H–O···H–N₁₄ complex being stable, and the N₃···H–O–H···O₇ structure converges to the former structure. The IR frequencies of the complex N₃···H–O–H···O₇ were calculated at the SCF/6-31G** level.

Results and Discussion

Tautomerism of 1MC. It is somewhat surprising that so few theoretical results have been published for such a biologically important nucleoside analogue of cytosine as 1MC.^{10,19,20} Table 1 summarizes the results of the *ab initio* MP2/6-31++G** calculations for the 1MC tautomers and includes a comparison to results published previously. It can be seen that all levels of theory used predict the a–o form as the most stable one. The energy difference with the *E* rotamer of the i–o form is 13.69 kJ mol^{–1} according to the MP2 calculation, which is considerably larger than in the earlier predictions using lower-level methods. An energy difference of about 14 kJ mol^{–1} would imply that about 2% of the compound occurs as the rare i–o form in the gas phase at the (body) temperature of 37 °C. It has been demonstrated that this amount is strongly dependent on environmental factors in the living cells.²¹ Katritzky and Karelson have used the semiempirical AM1 method to estimate the influence of the dielectric constant (ϵ) on the relative heats of formation of the 1MC tautomers, and they predicted an

TABLE 2: Experimental (Ar Matrix) and Calculated (SCF/6-31++G) IR Spectral Data for the Amino–Oxo Tautomer of 1-CH₃-Cytosine**

experimental		calculated (6-31++G**)		calculated ²⁴ (6-31G*)		PED ^e
ν (cm ⁻¹)	I^a (km/mol)	ν^c (cm ⁻¹)	I (km/mol)	ν^d (cm ⁻¹)	I (km/mol)	
3564/3558	62	3592	69	3534	60	$\nu^a(\text{NH}_2)$ (99)
3443/3437	96	3463	105	3419	97	$\nu^s(\text{NH}_2)$ (99)
3017	2	3063	3	3044	7	$\nu(\text{C}_5\text{H})$ (79) + $\nu(\text{C}_6\text{H})$ (20)
2997	2	3042	4	3025	4	$\nu(\text{C}_6\text{H})$ (79) + $\nu(\text{C}_5\text{H})$ (21)
2963	4	2977	15	2967	20	$\nu^d_1(\text{CH}_3)$ (100)
2954	5	2974	17	2961	17	$\nu^d_2(\text{CH}_3)$ (92)
2927	13	2900	49	2890	44	$\nu^s(\text{CH}_3)$ (92)
1717/1702/1691	340	1729	886	1743	774	$\nu(\text{C}=\text{O})$ (83)
1662/1654/1647	361	1659	778	1656	735	$\nu(\text{C}_5\text{C}_6)$ (34) + $\nu(\text{N}_3\text{C}_4)$ (20) + $\delta(\text{C}_6\text{H})$ (12)
1594	154	1607	154	1608	109	$\delta(\text{NH}_2)$ (81)
1539/1532	162	1536	382	1528	365	$\nu(\text{N}_3\text{C}_4)$ (26) + $\nu(\text{C}_4\text{C}_5)$ (18) + $\nu(\text{C}_5\text{C}_6)$ (15)
1491/1488	118	1485	76	1482	50	$\nu(\text{N}_3\text{C}_4)$ (16) + $\nu(\text{C}_6\text{N}_1)$ (12) + $\delta(\text{C}_5\text{H})$ (14) + $\delta^s(\text{CH}_3)$ (12)
1472	19	1472	22	1472	38	$\delta^d_1(\text{CH}_3)$ (73)
1430	10	1439	7	1446	4	$\delta^d_2(\text{CH}_3)$ (92)
1419	26	1430	21	1429	15	$\delta^s(\text{CH}_3)$ (85)
1369	113	1358	391	1353	377	$\nu(\text{C}_6\text{N}_1)$ (15) + $\nu(\text{C}_4\text{N})$ (14)
1324	5	1310	1	1305	3	$\delta(\text{C}_6\text{H})$ (41) + $\nu(\text{C}_4\text{N})$ (14)
1235	19	1244	18	1234	16	$\nu(\text{C}_2\text{N}_3)$ (35) + $\nu(\text{N}_1\text{C}_2)$ (13)
1214 or 1203	9	1196	12	1190	11	$\nu(\text{N}_1\text{C}_{10})$ (35) + $\delta(\text{C}_5\text{H})$ (21) + $\nu(\text{C}_5\text{C}_6)$ (14)
1144	47	1134	70	1129	67	$\delta(\text{C}_5\text{H})$ (23) + $\delta(\text{C}_6\text{H})$ (22) + $\rho_1(\text{CH}_3)$ (17)
1127	3	1127	2	1123	2	$\rho_2(\text{CH}_3)$ (90)
1076	38	1074	21	1072	25	$\rho(\text{NH}_2)$ (46)
1044	14	1039	13	1032	12	$\rho_1(\text{CH}_3)$ (35) + $\nu(\text{C}_6\text{N}_1)$ (17) + $\delta(\text{C}_5\text{H})$ (14) + δ_{R1} (11)
1001	8	995	1	986	0	$\gamma(\text{C}_6\text{H})$ (98) + $\gamma(\text{C}_5\text{H})$ (15)
948	5	939	3	933	3	$\nu(\text{C}_4\text{C}_5)$ (37) + $\rho(\text{NH}_2)$ (18) + $\nu(\text{N}_1\text{C}_2)$ (16) + δ_{R1} (11)
784	42	789	60	789	72	$\gamma(\text{C}_2\text{O})$ (86) + τ_{R1} (15)
763	29	768	36	762	30	δ_{R1} (24) + $\gamma(\text{C}_4\text{N})$ (20) + $\gamma(\text{C}_5\text{H})$ (20) + $\nu(\text{N}_1\text{C}_{10})$ (11)
747	8	763	14	755	34	$\gamma(\text{C}_5\text{H})$ (30) + $\gamma(\text{C}_4\text{N})$ (27) + δ_{R1} (17)
752	3	742	2	735	2	$\nu(\text{N}_1\text{C}_2)$ (30) + $\nu(\text{N}_1\text{C}_{10})$ (13) + $\nu(\text{N}_1\text{C}_6)$ (11)
710/708	36	704	11	704	4	$\gamma(\text{C}_5\text{H})$ (35) + $\gamma(\text{C}_4\text{N})$ (28) + τ_{R1} (20) + $\delta(\text{N}_1\text{C}_{10})$ (12)
611	2	597	4	592	3	δ_{R3} (41) + $\delta(\text{C}_2\text{O})$ (15) + $\delta(\text{C}_4\text{N})$ (13)
564	18	554	2	549	2	$\delta(\text{C}_2\text{O})$ (34) + δ_{R3} (32)
536	110	515	23	516	38	$\tau(\text{NH}_2)$ (83)
480	34	463	9	459	7	δ_{R2} (66) + $\nu(\text{N}_1\text{C}_{10})$ (11)
415	23	403	10	397	12	τ_{R2} (60) + τ_{R1} (24) + $\gamma(\text{C}_4\text{N})$ (13)
<i>b</i>		357	7	355	6	$\delta(\text{C}_4\text{N})$ (39) + $\delta(\text{C}_2=\text{O})$ (19) + $\delta(\text{N}_1\text{C}_{10})$ (17)
<i>b</i>		320	5	318	4	$\delta(\text{N}_1\text{C}_{10})$ (56) + $\delta(\text{C}_4\text{N})$ (26)
<i>b</i>		242	1	245	0	$\gamma(\text{N}_1\text{C}_{10})$ (59) + τ_{R1} (18)
<i>b</i>		180	6	184	1	τ_{R2} (32) + τ_{R1} (23) + $\gamma(\text{N}_1\text{C}_{10})$ (26)
<i>b</i>		141	261	198	335	wag (NH ₂) (90)
<i>b</i>		112	1	116	2	$\tau(\text{CH}_3)$ (73) + $\gamma(\text{N}_1\text{C}_{10})$ (28)
<i>b</i>		98	3	100	4	τ_{R3} (96) + $\tau(\text{CH}_3)$ (15)

^a Experimental intensities normalized to the calculated value of the $\delta(\text{NH}_2)$ mode (154 km/mol). ^b Situated below studied region. ^c Uniform scaling factor 0.90. ^d Uniform scaling factor 0.89. ^e Only contributions >10% are listed. ν designates stretching, δ in-plane deformation, γ out-of-plane deformation, ρ rocking, and τ torsion mode. The methyl stretches and in-plane deformations are further indicated by subscripts “d” (degenerate) and “s” (symmetric).

increase of the stability of the a–o tautomer by 6.2 and 27.0 kJ mol⁻¹ for $\epsilon = 1$ and $\epsilon = 80$, respectively.¹⁹ The decrease in the population of the rare i–o form in the more polar environment is expected from the difference between the dipole moments of the tautomers.²¹ The larger dipole moment of the a–o tautomer compared to the i–o *E* form is confirmed by the theoretical calculations (see Table 1). The energy difference between the a–o and both i–h forms is very large (82–97 kJ mol⁻¹), and this implies that identification of these forms in a low-temperature matrix is extremely improbable.

The energy values in Table 1 suggest that only the most intense vibrational modes of the i–o tautomer are observable in the matrix FT-IR spectrum of 1MC. The first matrix IR results for 1MC were reported by Szczesniak et al.²² and by Radchenko et al.²³ The former authors proved recently that the rare i–o *E* form is present in the Ar matrix and that this tautomer can be interconverted into the i–o *Z* rotamer using UV irradiation.¹⁰

Figure 1 shows the FT-IR spectrum of 1MC in Ar. Table 2 tabulates the experimental and theoretically predicted spectral parameters for the most abundant a–o tautomer. The mean

difference between the experimental and predicted frequencies is 12.8 cm⁻¹, while the predicted intensities are, with the exception of a few values only, largely in qualitative agreement with the experimental values. Our main interest here is to assign the H-bond sensitive vibrational modes of the NH₂-group (ν^a -(NH₂), ν^s -(NH₂), ρ -(NH₂), and τ -(NH₂)). Close correspondence between the theoretical and experimental spectral parameters allows us to assign these modes to the experimental absorption bands observed at 3558, 3437, 1076, and 536 cm⁻¹, respectively. Contrary to our earlier observations made for 4-NH₂-pyridine and 4-NH₂-pyrimidine,² the correspondence between the experimental and predicted intensity values of the NH₂ stretching modes in 1MC is quite good. The modes to be used as probes of the H-bond interaction at the C₂=O site are the $\nu(\text{C}_2=\text{O})$ mode assigned to the band at 1717 cm⁻¹ and the $\gamma(\text{C}_2=\text{O})$ mode assigned to the absorption found at 784 cm⁻¹. Table 2 also lists the SCF/6-31G* predicted frequencies and intensities taken from a recent report of Person and Szczepaniak,²⁴ and it appears that the predictions at the two levels of theory are largely consistent. As a matter of fact, almost no further improvement

TABLE 3: Experimental (Ar Matrix) and Calculated (SCF/6-31++G) IR Spectral Data for the Imino-oxo *E* Tautomer of 1-CH₃-Cytosine**

experimental		calculated		PED ^f
ν (cm ⁻¹)	I^a (km/mol)	ν^e (cm ⁻¹)	I (km/mol)	
<i>b</i>		3477	87	$\nu(\text{N}_3\text{H})$ (100)
<i>b</i>		3411	15	$\nu(\text{N}_{14}\text{H})$ (102)
<i>b</i>		3068	3	$\nu(\text{C}_5\text{H})$ (66) + $\nu(\text{C}_6\text{H})$ (33)
<i>b</i>		3050	2	$\nu(\text{C}_6\text{H})$ (66) + $\nu(\text{C}_5\text{H})$ (33)
<i>b</i>		2980	17	$\nu^{\text{d}_1}(\text{CH}_3)$ (101)
<i>b</i>		2973	17	$\nu^{\text{d}_2}(\text{CH}_3)$ (100)
<i>b</i>		2901	49	$\nu^s(\text{CH}_3)$ (101)
1758/1732	473	1746	933	$\nu(\text{C}_2\text{O})$ (74)
1674	300	1705	917	$\nu(\text{C}_4\text{N}_{14})$ (48) + $\nu(\text{C}_5\text{C}_6)$ (16)
<i>b</i>		1639	8	$\nu(\text{C}_5\text{C}_6)$ (44) + $\nu(\text{C}_4\text{N}_{14})$ (24)
1477	<i>d</i>	1482	52	$\delta^{\text{d}_1}(\text{CH}_3)$ (78)
1455	27	1454	61	$\delta^s(\text{CH}_3)$ (27) + $\nu(\text{N}_3\text{C}_4)$ (11)
1443	27	1444	66	$\delta^s(\text{CH}_3)$ (54)
<i>b</i>		1443	7	$\delta^{\text{d}_2}(\text{CH}_3)$ (92)
1393	72	1399	189	$\delta^s(\text{CH}_3)$ (18) + $\delta(\text{C}_5\text{H})$ (15) + $\nu(\text{C}_2\text{N}_3)$ (14)
<i>b</i>		1396	26	$\delta(\text{N}_3\text{H})$ (46) + $\nu(\text{C}_4\text{N}_{14})$ (14) + $\delta(\text{C}_6\text{H})$ (12)
1324	102	1318	137	$\nu(\text{C}_6\text{N}_1)$ (25) + $\delta(\text{C}_4\text{N}_{14})$ (21) + $\rho_1(\text{CH}_3)$ (17)
1284	39	1284	43	$\nu(\text{C}_2\text{N}_3)$ (17) + $\delta(\text{N}_{14}\text{H})$ (14) + $\nu(\text{N}_1\text{C}_2)$ (12) + $\delta(\text{C}_6\text{H})$ (12) + $\delta(\text{N}_3\text{H})$ (11)
<i>b</i>		1194	11	$\nu(\text{N}_1\text{C}_{10})$ (34) + $\nu(\text{C}_2\text{N}_3)$ (18) + $\delta_{\text{R}1}$ (15) + $\delta(\text{C}_5\text{H})$ (14)
<i>b</i>		1151	6	$\delta(\text{C}_5\text{H})$ (30) + $\delta(\text{C}_6\text{H})$ (20) + $\rho_1(\text{CH}_3)$ (17)
<i>b</i>		1127	2	$\rho_2(\text{CH}_3)$ (91)
1115	213	1109	213	$\delta(\text{N}_{14}\text{H})$ (53) + $\nu(\text{N}_3\text{C}_4)$ (15) + $\rho_1(\text{CH}_3)$ (11)
<i>b</i>		1025	18	$\nu(\text{C}_6\text{N}_1)$ (21) + $\rho_1(\text{CH}_3)$ (34)
<i>b</i>		984	1	$\gamma(\text{C}_6\text{H})$ (92) + $\gamma(\text{C}_5\text{H})$ (24)
<i>b</i>		951	2	$\nu(\text{C}_4\text{C}_5)$ (28) + $\delta_{\text{R}1}$ (20) + $\nu(\text{N}_1\text{C}_2)$ (14)
813	101	827	119	$\gamma(\text{N}_{14}\text{H})$ (52) + $\gamma(\text{C}_4\text{N})$ (30) + $\gamma(\text{C}_5\text{H})$ (15)
<i>b</i>		775	6	$\delta_{\text{R}1}$ (41) + $\nu(\text{N}_1\text{C}_{10})$ (23) + $\nu(\text{C}_4\text{C}_5)$ (12)
<i>b</i>		772	19	$\gamma(\text{C}_2\text{O})$ (79) + $\gamma(\text{C}_5\text{H})$ (13)
<i>b</i>		745	52	$\gamma(\text{N}_{14}\text{H})$ (40) + $\gamma(\text{C}_5\text{H})$ (38) + $\gamma(\text{C}_2\text{O})$ (23)
<i>b</i>		725	12	$\nu(\text{N}_1\text{C}_2)$ (27) + $\nu(\text{C}_4\text{C}_5)$ (16) + $\nu(\text{C}_6\text{N}_1)$ (13) + $\nu(\text{N}_1\text{C}_{10})$ (14)
<i>b</i>		680	0	$\gamma(\text{C}_4\text{N})$ (48) + $\tau_{\text{R}1}$ (28) + $\gamma(\text{C}_5\text{H})$ (12)
629	178	612	102	$\gamma(\text{N}_3\text{H})$ (97)
<i>b</i>		600	8	$\delta_{\text{R}3}$ (34) + $\delta(\text{C}_4\text{N})$ (13) + $\nu(\text{C}_6\text{N}_1)$ (14) + $\delta(\text{C}_2\text{O})$ (12) + $\delta(\text{N}_1\text{C}_{10})$ (13)
<i>b</i>		537	11	$\delta_{\text{R}3}$ (31) + $\delta(\text{C}_2\text{O})$ (28)
<i>b</i>		452	32	$\delta_{\text{R}2}$ (66)
<i>c</i>		387	7	$\tau_{\text{R}2}$ (64) + $\tau_{\text{R}1}$ (24) + $\gamma(\text{C}_4\text{N})$ (19)
<i>c</i>		369	14	$\delta(\text{C}_4\text{N})$ (44) + $\delta(\text{C}_2\text{O})$ (23)
<i>c</i>		319	5	$\delta(\text{N}_1\text{C}_{10})$ (72)
<i>c</i>		192	4	$\gamma(\text{N}_1\text{C}_{10})$ (83) + $\tau_{\text{R}3}$ (12)
<i>c</i>		151	0	$\tau_{\text{R}1}$ (58) + $\tau_{\text{R}2}$ (26) + $\tau_{\text{R}3}$ (32)
<i>c</i>		92	0	$\tau_{\text{R}3}$ (65) + $\tau_{\text{R}2}$ (28)
<i>c</i>		44	0	$\tau(\text{CH}_3)$ (89) + $\gamma(\text{N}_1\text{C}_{10})$ (17)

^a Experimental intensities normalized to the calculated value of the $\delta(\text{N}_{14}\text{H})$ mode (213 km/mol). ^b Too weak to be observed. ^c Situated below studied region. ^d Too close to an intense mode of the a-o tautomer. ^e Uniform scaling factor 0.90. ^f See Table 2.

in frequency prediction accuracy is obtained with the 6-31++G** basis set compared to the 6-31G* basis set for monomeric compounds.

Some of the weak absorptions in the experimental spectrum of 1MC/Ar, which cannot be assigned to the a-o tautomer (Table 2), *e.g.*, those at 1115 or 813 cm⁻¹, can be attributed to the rare i-o *E* form. This is clear from a detailed comparison of the experimental absorptions to the *ab initio* predicted modes of the i-o *E* form (Table 3). The assignment of the experimental bands to the latter tautomer is performed using several leads. First of all, only those absorptions of the i-o form that have a large predicted intensity should be observed experimentally. Some of the weak IR bands are located relatively far from the predicted frequencies for the a-o tautomer, *e.g.*, the absorption at 1284 cm⁻¹ is far from the predicted a-o frequencies of 1310 or 1244 cm⁻¹, which leaves little doubt about their origin from the i-o form. In cases where i-o band frequencies are predicted to be close to a-o frequencies, the intensity predictions are used as a guide for assigning the bands to the i-o *E* form. The last, but important, guide for the assignment of the absorptions originating from the rare i-o tautomer is that these bands agree very well with the bands

TABLE 4: Experimental Estimation of the K_T (a-o/i-o *E*) value for 1-CH₃-Cytosine in Ar

band pair (amino-oxo/imino-oxo) $\nu_{\text{ao}}(\text{cm}^{-1})/\nu_{\text{io}}(\text{cm}^{-1})$	K_T (a-o/i-o <i>E</i>) (75 °C)
1717–1702–1691 $\nu(\text{C}=\text{O})$ /1758–1732 $\nu(\text{C}=\text{O})$	5.0
1662–1654–1647 $\nu(\text{C}_5=\text{C}_6)$ /1674 $\nu(\text{C}_4=\text{N}_{14})$	6.7
1369 $\nu(\text{C}_6\text{N}_1)$ /1393 $\delta^s(\text{CH}_3)$	8.4
1369 $\nu(\text{C}_6\text{N}_1)$ /1324 $\nu(\text{C}_6\text{N}_1)$	6.9
1235 $\nu(\text{C}_2\text{N}_3)$ /1284 $\nu(\text{C}_2\text{N}_3)$	11.6
1144 $\delta(\text{C}_5\text{H})$ /1115 $\delta(\text{N}_{14}\text{H})$	6.4
784 $\gamma(\text{C}_2\text{O})$ /813 $\gamma(\text{N}_{14}\text{H})$	5.1
mean value (75 °C)	7.2 ± 2.3
literature value (190 °C) ¹⁰	6.7 ± 0.15

shown in Figure 1 of ref 10, and those were independently proven to originate from the modes of the i-o *E* form.¹⁰

The tautomerization constant K_T (a-o/i-o *E*) can be estimated using the experimental integrated intensities and calculated absorption coefficients of characteristic modes of the two respective tautomers.^{5,6,25–27} The number of characteristic modes is limited because some of the i-o *E* bands are too weak, *e.g.*, the bands at 1455 or 1443 cm⁻¹, while others show a broadened profile indicating overlap with some other bands,

CHART 2

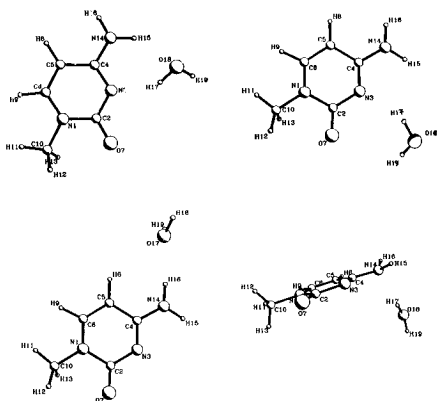
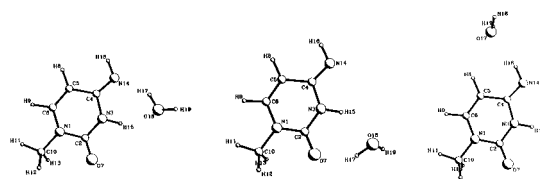


CHART 3



e.g., the band at 629 cm^{-1} . Table 4 lists the estimated values of $K_T(\text{a-o/i-o } E)$ obtained in this work. The rather large deviations observed between individual K_T estimations are due to the experimental inaccuracy of the (weak) band intensity measurements and to errors in the predicted absorption coefficients. It is, therefore, possible to estimate only the order of magnitude of the constant K_T . Nevertheless, the mean value of 7.2 is relatively close to the value of 6.7 reported by Szczesniak et al.¹⁰ although theoretical absorption coefficients predicted at different levels of theory were used in the two cases. This K_T value allows one to estimate the standard free enthalpy difference, ΔG° , at 348 K:

$$\Delta G^\circ(\text{a-o/i-o } E) = -RT \ln K_T(\text{a-o/i-o } E) = -5.7\text{ kJ mol}^{-1}$$

This value can be compared to the values of the MP2 and SCF energy differences, ΔE , of -13.7 and -8.4 kJ mol^{-1} . Such comparison is often made, and theory seems to reproduce the energy difference between tautomers of nucleic acid bases rather well, especially when electron-correlation is taken into account.²⁷ However, two remarks about the comparison of the experimental $\Delta G^\circ(T)$ and the theoretical $\Delta E(0\text{ K})$ values must be made. The first one concerns the underlying assumption that the temperature-dependent contributions $\delta\Delta H^\circ/\delta T$ and $T\Delta S^\circ$ to the relative free enthalpy difference can be neglected. Kwiatkowski and Leszczynski have recently demonstrated that the sum of the two contributions amounts to a maximum of about 1.5 kJ mol^{-1} for amino \rightleftharpoons imino tautomerism in adenine,²⁸ which indicates that this assumption is quite acceptable. A more serious question is whether the experimental $\Delta G^\circ(T)$ and the theoretical $\Delta E(0\text{ K})$ values can be compared at all, since proton transfer involved in the process of tautomer interconversion is probably not monomolecular and not only thermodynamic but also kinetic factors determine the relative concentration of the tautomers in the matrix. As a matter of fact, the barrier for intramolecular proton transfer estimated at the CISD level has been demonstrated to be as large as 161 kJ mol^{-1} for hydroxy \rightleftharpoons oxo tautomerism in 2-OH-pyridine.²⁹ This barrier drastically decreases when one or more water molecules are bonded to 2-OH-pyridine or in the dimeric form. A barrier of only 60 kJ mol^{-1} has been calculated for a concerted, biprotonic tautomerization

TABLE 5: Calculated (SCF/6-31++G**) Spectral Data for the Imino-Oxo Z, Imino-Hydroxy E, and Imino-Hydroxy Z Tautomers of 1-CH₃-Cytosine

imino-oxo Z		imino-hydroxy E		imino-hydroxy Z	
ν^a (cm ⁻¹)	I (km/mol)	ν^a (cm ⁻¹)	I (km/mol)	ν^a (cm ⁻¹)	I (km/mol)
3478	60	3716	167	3723	161
3377	11	3384	7	3384	12
3086	2	3063	7	3076	3
3057	5	3040	0.2	3057	2
2981	17	2980	17	2982	16
2971	18	2966	20	2965	21
2901	49	2898	58	2898	58
1742	927	1703	1075	1703	1029
1712	809	1676	82	1675	12
1649	8	1583	416	1586	426
1481	41	1497	267	1501	317
1450	41	1469	59	1469	71
1444	7	1449	7	1450	7
1437	142	1445	46	1447	36
1410	43	1396	15	1398	47
1394	123	1332	69	1314	23
1315	89	1296	45	1292	61
1270	192	1242	49	1239	164
1186	8	1210	141	1209	116
1148	58	1150	13	1148	54
1127	2	1124	2	1124	1
1103	35	1099	252	1104	100
1017	53	1017	2	1010	15
982	1	972	0.1	973	1
954	18	938	13	936	15
832	67	853	119	883	71
784	22	775	8	799	61
777	12	764	20	761	31
761	130	750	48	751	35
727	5	724	12	727	6
674	13	679	11	675	31
599	11	582	8	580	19
556	53	534	9	526	12
534	3	530	115	517	113
451	14	475	19	469	7
384	23	405	0.4	400	10
369	50	364	14	359	14
318	1	320	1	321	2
190	2	212	8	213	1
153	3	172	4	175	4
91	0	74	0.2	80	0
22	0	45	0.7	37	0

^a Uniform scaling factor 0.90.

in the 2-OH-pyridine dimer at the SCF level.²⁹⁻³¹ This suggests that the tautomeric equilibrium in the gas phase is probably not governed by the free enthalpy difference between the monomeric tautomers. The thermodynamic quantities estimated from the experiment reflect a temperature-dependent stationary state achieved in a more complicated process in which formation and dissociation of short-living dimers are involved. Despite the above arguments, recent studies have demonstrated that *ab initio* energy calculations using extended basis sets such as 6-31G** or better, including electron-correlation effects beyond the second order, reproduce the order of magnitude of the stability difference between tautomers rather well.³²

The *ab initio* predicted frequencies and intensities for the i-o Z form and the two i-h rotamers E and Z are listed in Table 5. A comparison of the optimized geometries of the a-o tautomer at the 6-31G*²⁴ and the 6-31++G** (this work) levels can be made. All differences between bond distances are within $2 \times 10^{-3}\text{ \AA}$, and those for bond angles are within 0.5° . The dipole moment calculated at the 6-31++G** level is 6.97 D, and this value can be compared to the experimental value of 6.2 D for 1-cyclohexylcytosine.³³

Hydrogen-Bonded Complexes 1MC·H₂O. The abundant a-o tautomer of 1MC has three proton-acceptor sites (C₂=O,

TABLE 6: Ab Initio 6-31G++G Predicted Energy Components (au), Total Energies (kJ/mol), Interaction Energies, and Interaction Energies Corrected for the Basis Set Superposition Error (kJ/mol) for H-Bonded Complexes of Water with the a-o Tautomer of 1-CH₃-Cytosine^e**

method	N ₃ ...H-O...H-N ₁₄		N ₃ ...H-O-H...O ₇ =C ₂	N ₁₄ -H...OH ₂	N ₁₄ ...H-OH
	a	b	a	a	a
SCF	-507.721 451 4	-507.714 552 2	-507.718 465 0	-507.714 904 5	-507.711 342 8
MP2 ^a	-509.266 003 3	-509.272 287 15	-509.260 903 6	-509.257 777 7	-509.255 647 3
SCF (base with ghost water orbitals)	-431.675 351 9		-431.675 331 6	-431.675 182 4	
MP2 (base with ghost water orbitals)	-433.015 005 8		-433.014 902 2	-433.014 453 9	
SCF (water with ghost base orbitals)	-76.032 014 0		-76.032 075 0	-76.031 891 5	
MP2 (water with ghost base orbitals)	-76.234 546 2		-76.234 361 7	-76.234 429 0	
ZPE ^b		0.146 058 6	0.145 826 3 ^d	0.145 037 7	0.145 514 7
total	-509.119 944 7	-509.126 228 6	-509.115 077 3	-509.112 724 0	-509.110 130 0
ΔE _T ^c	0.0	0.0	12.78	18.95	25.77
interaction energy (SCF + ZPE)	-30.98		-23.75	-16.48	-5.87
interaction energy (SCF/BSSE + ZPE)	-28.33		-20.99	-14.59	
interaction energy (MP2 + ZPE)	-43.13		-30.35	-24.17	-17.36
interaction energy (MP2/BSSE + ZPE)	-34.54		-22.52	-17.34	
μ (D)	6.16		9.31	9.56	5.09

^a Only valence correlation is considered. ^b Calculated as $0.9\sum hv/2$. ^c Energy difference between isomeric complexes. ^d Calculated with the 6-31G** basis set. ^e Geometry optimization at the SCF/6-31++G** (a), the MP2/6-31++G** (b), or the SCF/6-31G** (c) level; all calculations performed at the 6-31++G** level.

N₃, and N₁₄), whereas the amino group probably acts only as a proton donor, as suggested by our studies on water complexes of 4-NH₂-pyridine and 4-NH₂-pyrimidine.² On the other hand, the rare but experimentally observed i-o *E* tautomer has one less proton-acceptor site (N₃) but one more proton-donor site (N₃H). Charts 2 and 3 show the optimized structures of the water complexes of the a-o and i-o *E* tautomers, respectively, obtained at the SCF/6-31++G** level (the N₃...H-OH...O₇ structure of the a-o tautomer was obtained at the SCF/6-31G** level). We will further comment on geometry differences between the optimized structures at this and at the MP2 level of theory used for the N₃...H-O...H-N₁₄ complex of a-o IMC.

Table 6 summarizes the energy calculations for the four *ab initio* predicted stable water complexes of a-o IMC. At both the SCF/6-31++G** and MP2/6-31++G** levels of theory, the closed N₃...H-O...H-N₁₄ structure is by far the most stable one among these complex structures. A similar, closed H-bonded structure showing significant H-bond cooperativity has been observed for 4-NH₂-pyrimidine (4APM), and the theoretical calculations indicated that this complex is also significantly more stable than the open N-H...OH₂ structure by about 10 kJ mol⁻¹.² The stability differences of the a-o IMC N₃...H-O...H-N₁₄ structure and the alternative closed but anticooperative N₃...H-O-H...O₇ complex, which has been observed as the most stable complex for 1-CH₃-2-pyrimidone (MOP) and *N,N*-1-triCH₃-cytosine (TMC) at the SCF/6-31++G** optimization level,⁴ amounts to 12.78 kJ mol⁻¹ at the SCF optimization level, which is a relatively large stability difference. The N₃...O H-bond in the N₃...H-O-H...O₇ structure of a-o IMC appears to be shorter (3.115 Å) than the H-bond O...O₇ (3.170 Å) at the SCF optimization level, indicating the inequivalency of the H-bonds present in this more or less "bifurcated" complex. On the other hand, the open N₁₄-H...OH₂ and N₁₄...H-OH structures are still less stable by 18.95 and 25.77 kJ mol⁻¹, respectively. The interaction energies calculated at the MP2/BSSE+ZPE level for the four complexes also decrease in the same order. It is worth noting that the (SCF optimized) interaction energy of the strongest, cooperative closed N₃...H-O...H-N₁₄ complex is noticeably larger (-34.54 kJ mol⁻¹) than for the similar complex of 4APM (-25.98 kJ mol⁻¹).² This is also reflected by the N₃...O and the O...N₁₄ distances, which are shorter in the complex with a-o IMC (2.923 and 3.039 Å) than in the complex with 4APM (2.978 and 3.062 Å). A stronger H-bond at the N₃ atom is obviously due to a larger proton affinity of this site in IMC (935 kJ mol⁻¹ in cytosine).

TABLE 7: Ab Initio 6-31G+ +G Predicted Energy Components (au), Total Energies (kJ/mol), and Interaction Energies (kJ/mol) for the H-Bonded Complexes of Water with the i-o *E* Tautomer of 1-CH₃-Cytosine**

method	N ₁₄ ...H-O...H-N ₃	O ₇ ...H-O...H-N ₃	N ₁₄ -H...OH ₂
SCF	-507.716 641 1	-507.714 817 0	-507.709 619 9
MP2 ^a	-509.259 649 0	-509.256 833 6	-509.250 198 8
ZPE ^b	0.147 036 4	0.146 679 9	0.145 613 0
total	-509.112 612 6	-509.110 153 7	-509.104 585 8
ΔE _T ^c	0.0	6.46	21.07
ΔE _T ^d	19.25	25.71	40.32
interaction energy (SCF + ZPE)	-23.93	-20.29	-9.44
interaction energy (MP2 + ZPE)	-37.54	-31.08	-23.51
μ (D)	6.06	5.73	6.32

^a Only valence correlation is considered. ^b Calculated as $0.9\sum hv/2$. ^c Energy difference between isomeric complexes. ^d Energy difference with the most stable N₃...H-O...H-N₁₄ complex of the amino-oxo tautomer.

The more acidic character of the amino N-H bonds in a-o IMC is manifested by a larger interaction energy (-17.34 kJ mol⁻¹) of the N₁₄-H...OH₂ complex compared to the interaction energy in the similar complex of 4APM (-16.26 kJ mol⁻¹).² Comparison of the interaction energy of the closed H-bonded N₃...H-O-H...O₇ complex of IMC to that of similar structures predicted at the SCF/6-31++G** level for MOP and TMC⁴ is more approximate, since this structure is only found with the basis set 6-31G** at the SCF optimization level for a-o IMC. Nevertheless, the interaction energy in the IMC complex is of the same order of magnitude as for the MOP and TMC complexes. The N₃...H distances are 2.308, 2.178, and 2.199 Å for the complexes of MOP, TMC, and IMC, respectively, which indicates a definite similarity between the H-bonds in the latter two compounds. However, a decreasing degree of O-H...O₇ bonding appears in the closed structures within the series MOP → IMC → TMC as manifested by the increasing O₇...H distance (2.562 → 2.640 → 3.013 Å).

Table 7 summarizes the energy calculations for three stable complexes of water with the i-o *E* form of IMC. In this case, the N₁₄...H-O...H-N₃ complex is predicted to be the most stable with the energy differences with the alternative closed O₇...H-O...H-N₃ and open N₁₄-H...OH₂ structures being 6.46 and 21.07 kJ mol⁻¹, respectively. A comparison to the results in Table 1 allows us to conclude that the energy difference between the a-o and i-o *E* tautomers increases from 13.69 to 19.25 kJ mol⁻¹ because of H-bonding with water. This

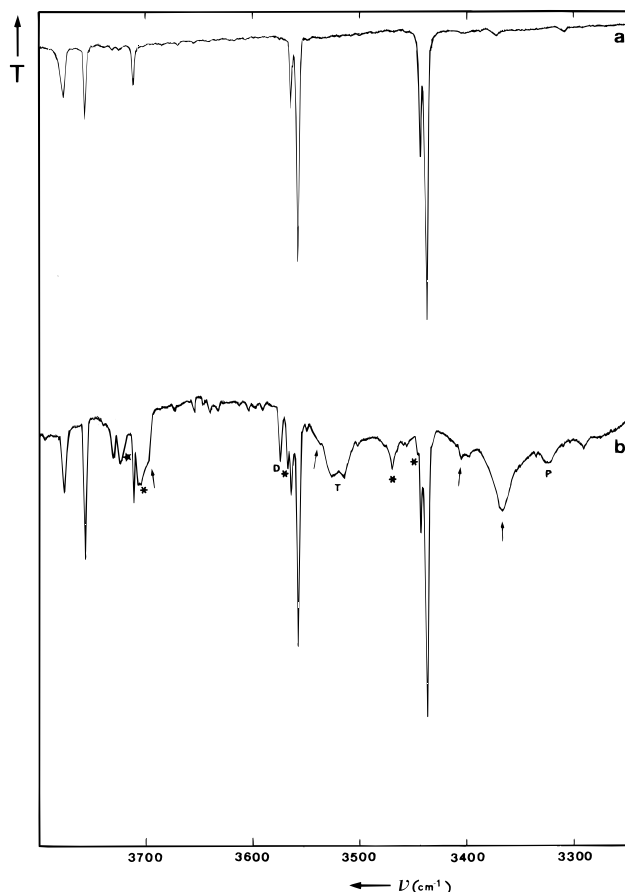


Figure 2. High-frequency region of the FT-IR spectrum of 1-CH₃-cytosine/H₂O/Ar at 12 K ((a) H₂O/Ar = impurity level; (b) H₂O/Ar = 1/500): † = N₃...H-O...H-N₁₄ complex of a-o form; * = C₂=O...HO-H complex of a-o form; ★ = N₁₄-H...OH₂ complex (tentative); D, T, P = water dimer, trimer, polymer.

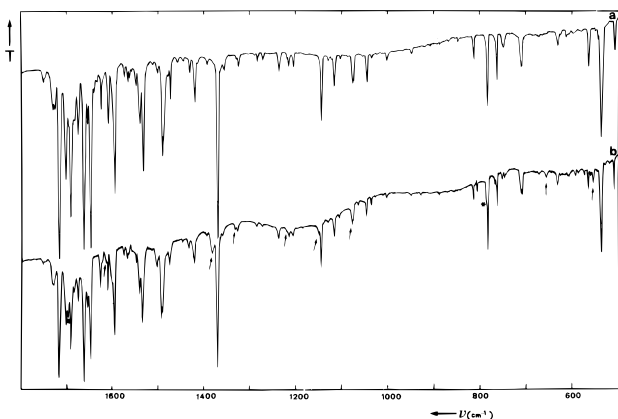


Figure 3. Fingerprint region of the FT-IR spectrum of 1-CH₃-cytosine (a) and of 1-CH₃-cytosine/H₂O/Ar (b) at 12 K († and * are defined as in Figure 2).

observation, which is consistent with the AM1 results of Katritzky and Karelson mentioned earlier,¹⁹ would imply that the abundance of the IMC a-o tautomer in the Ar matrix should slightly increase because of complexation of IMC with water.

Figures 2 and 3 illustrate the FT-IR spectra of IMC/H₂O/Ar. Our earlier results obtained for 4APM (coexistence of closed N₃...H-O...H-N and open N-H...OH₂ structures)² and for MOP and TMC (open N₃...H-O and O₇...H-O structures were found experimentally in contrast with the SCF/6-31++G** predicted closed structure N₃...H-O-H...O₇, but in slightly better accordance with the MP2/6-311++G** predictions)⁴ can be used for the interpretation of the spectra. The most relevant spectral changes are observed in the high-frequency region

(Figure 2). New absorptions appear in the water ν₃ region at 3704 and 3699 cm⁻¹ and in the ν₁ region at 3469 and 3350 cm⁻¹. Furthermore, shifted ν(NH₂) modes appear at 3539 (-18) cm⁻¹ (ν^a) and at 3404 (-33) cm⁻¹ (ν^s). In the fingerprint region (Figure 3), several complex bands appear near IMC monomer absorptions, the most important being the shifted ν(C=O) band at 1696 (-18) cm⁻¹, a new ν(C₄-N) absorption at 1381 (+12) cm⁻¹, and a shifted ν(N₃C₄) band at 1542 (+6) cm⁻¹. At last, two new bands are observed at 655 and 572 cm⁻¹.

In view of the large abundance of the a-o tautomer, the most intense absorptions should be assigned to one of the stable H-bonded structures of this form. The observed spectral perturbations seem to manifest the presence of at least two different H-bonded complexes of the IMC a-o tautomer in Ar, most probably the closed N₃...H-O...H-N₁₄ structure and the open O₇...H-OH complex. By use of the results obtained for 4APM·H₂O, the closed N₃...H-O...H-N₁₄ complex is expected to be characterized by a large shift of the ν^b_{OH} mode,² and this is an argument for the assignment of the most intense complex band observed at 3350 cm⁻¹ to this mode. Further characteristic bands of this structure are the ν^f_{OH} mode at 3699 cm⁻¹ and the frequency-decreased amino stretches ν^a (-18 cm⁻¹) and ν^s (-33 cm⁻¹). The corresponding shifts are consistent with the *ab initio* predictions listed in Table 8. The water stretching modes are more shifted in this case than for the weaker N₃...H-O...H-N complex of 4APM (-34/-286 cm⁻¹).²

An important new band manifesting the presence of the cooperative closed N₃...H-O...H-N₁₄ complex is the frequency-increased (+12 cm⁻¹) ν(C₄N₁₄) mode, also in accordance with the *ab initio* predictions. This band is predicted to be very intense in the closed complex, which implies that it already should appear in spectra of samples with low amounts of complex species. A comparison of Table 8 with Table 9, the latter summarizing the most relevant spectral perturbations of the other three complexes of the a-o tautomer, demonstrates that such a large positive shift of this mode is only predicted for the N₃...H-O...H-N₁₄ complex and not for the two other complexes involving the NH₂ group. Following the *ab initio* predicted shifts, a small frequency decrease of the ν(C=O) mode should be observed for the closed N₃...H-O...H-N₁₄ complex, but this shift is probably too small to be observed near this very intense monomer absorption in the experimental spectrum. On the other hand, the predicted, large shifts of the amino bending, rocking, torsion, and wagging modes are clearly observed (Table 9). The complex bands found at 655 and 572 cm⁻¹ are most probably of the same types as those observed for the closed complex N...H-O...H-N of water with 4APM, and they are therefore assigned to the upward-shifted τ(NH₂) and to a torsion mode of the water molecule, respectively.

Of the two predicted open complexes of the a-o tautomer, the N₁₄...H-OH structure should not be observable in the experimental spectrum. This was already the case for 4APM,² and this type of complex is predicted to be even less stable for a-o IMC. On the contrary, the occurrence of a small amount of the open N₁₄-H...OH₂ species cannot be excluded, and the experimental spectrum has been carefully analyzed in order to identify any of the characteristic water complex bands or shifts of the amino modes predicted for this structure (Table 9). In the case of 4APM, the presence of the open N-H...OH₂ structure has been argued from the observation of the water ν₃ and ν₂ bands at 3724 and 1594 cm⁻¹, close to the corresponding frequencies of the acceptor unit in the (H₂O)₂ dimer,³⁴ as well as from a strong, frequency-increased amino torsion mode.² In the case of a-o IMC, the situation is less clear, since a slightly increased water ν₂ absorption will be hidden by other intense

TABLE 8: Experimental (Ar Matrix) and Calculated (SCF/6-31++G) IR Spectral Data for the Closed N₃...H-O...H-N₁₄ H-Bonded Complex of a-o 1-CH₃-Cytosine with Water**

experimental		calculated			optimal scaling ^a	PED ^d
ν (cm ⁻¹)	$\Delta\nu$ (cm ⁻¹)	ν^a (cm ⁻¹)	I (km/mol)	$\Delta\nu$ (cm ⁻¹)		
water modes						
3699	-35	4235	150	-32	0.873	$\nu^f(\text{OH})(74) + \nu^b(\text{OH})(26)$
3350	-323	3998	419	-148	0.838	$\nu^b(\text{OH})(72) + \nu^f(\text{OH})(25)$
overlap		1756	77	+26	0.922	$\delta(\text{H}_2\text{O})(98)$
base modes						
572?		605	83			$\tau_2(\dots\text{OHH}\dots)(69)$
c		435	107			$\tau_1(\dots\text{OHH}\dots)(94) + \gamma(\text{C}_4\text{N})(16)$
c		154	4			$\nu^s(\text{H}\dots\text{O}-\text{H}\dots\text{N})(92)$
c		120	135			$\delta(\dots\text{OHH}\dots)(56) + \tau_1(\dots\text{OHH}\dots)(33)$
c		91	23			$\nu^a(\text{H}\dots\text{O}-\text{H}\dots\text{N})(77)$
c		39	8			$\gamma(\dots\text{HHO}\dots)(102)$
Base Modes						
3539	-18	3574	86	-18		$\nu^a(\text{NH}_2)(86) + \nu^s(\text{NH}_2)(11)$
3404	-33	3414	202	-50		$\nu^s(\text{NH}_2)(89) + \nu^a(\text{NH}_2)(10)$
b		3064	3	+1		$\nu(\text{C}_5\text{H})(78) + \nu(\text{C}_6\text{H})(21)$
b		3044	4	+2		$\nu(\text{C}_6\text{H})(78) + \nu(\text{C}_5\text{H})(21)$
b		2977	15	0		$\nu^{\text{d}_1}(\text{CH}_3)(93)$
b		2975	17	+1		$\nu^{\text{d}_2}(\text{CH}_3)(86)$
2929	+2	2900	49	0		$\nu^s(\text{CH}_3)(93)$
?		1725	875	-4		$\nu(\text{C}=\text{O})(74)$
1662	0	1659	896	0		$\nu(\text{C}_5\text{C}_6)(29) + \nu(\text{N}_3\text{C}_4)(14) + \delta(\text{NH}_2)(17)$
1612	+18	1628	22	+21		$\delta(\text{NH}_2)(65)$
1527	-5	1532	409	-4		$\nu(\text{N}_3\text{C}_4)(23) + \nu(\text{C}_4\text{C}_5)(20) + \nu(\text{C}_5\text{C}_6)(11)$
1491	0	1485	124	0		$\nu(\text{N}_3\text{C}_4)(19) + \delta(\text{C}_5\text{H})(14) + \nu(\text{C}_4\text{N})(13) + \delta^s(\text{CH}_3)(12) + \delta(\text{C}_6\text{H})(12)$
1475	+3	1474	22	+2		$\delta^{\text{d}_1}(\text{CH}_3)(79)$
b		1439	7	0		$\delta^{\text{d}_2}(\text{CH}_3)(92)$
1421	+2	1432	25	+2		$\delta^s(\text{CH}_3)(83)$
1381	+12	1369	382	+11		$\nu(\text{C}_4\text{N})(17) + \nu(\text{C}_6\text{N}_1)(17)$
1329	+5	1315	12	+5		$\delta(\text{C}_6\text{H})(42) + \delta(\text{C}_6\text{N}_1)(13)$
b		1252	20	+8		$\nu(\text{C}_2\text{N}_3)(35) + \nu(\text{N}_1\text{C}_2)(14) + \nu(\text{N}_3\text{C}_4)(12)$
1217	+3	1200	13	+4		$\nu(\text{N}_1\text{C}_{10})(35) + \delta(\text{C}_5\text{H})(16) + \delta(\text{C}_6\text{H})(22)$
1148	+4	1138	67	+4		$\delta(\text{C}_5\text{H})(25) + \delta(\text{C}_6\text{H})(22) + \rho_1(\text{CH}_3)(16)$
b		1127	2	0		$\rho_2(\text{CH}_3)(90)$
1084	+8	1091	22	+17		$\rho(\text{NH}_2)(47)$
1045	+1	1040	13	+1		$\rho_1(\text{CH}_3)(34) + \nu(\text{C}_6\text{N}_1)(17) + \delta(\text{C}_5\text{H})(14) + \delta_{\text{R}1}(11)$
b		995	1	0		$\gamma(\text{C}_6\text{H})(98) + \gamma(\text{C}_5\text{H})(15)$
b		950	5	+11		$\nu(\text{C}_4\text{C}_5)(38) + \rho(\text{NH}_2)(14) + \nu(\text{N}_1\text{C}_2)(17)$
783	-1	787	63	-2		$\gamma(\text{C}_2\text{O})(87) + \tau_{\text{R}1}(15)$
b		770	5	+2		$\delta_{\text{R}1}(40) + \gamma(\text{C}_4\text{N})(13) + \nu(\text{N}_1\text{C}_{10})(25)$
b		768	57	+5		$\gamma(\text{C}_5\text{H})(51) + \gamma(\text{C}_4\text{N})(46)$
b		746	1	+4		$\nu(\text{N}_1\text{C}_2)(30) + \nu(\text{C}_4\text{C}_5)(15)$
b		711	1	+7		$\gamma(\text{C}_5\text{H})(30) + \gamma(\text{C}_4\text{N})(26) + \tau_{\text{R}1}(18) + \tau(\text{NH}_2)(12)$
655	+119	663	154	+148		$\tau(\text{NH}_2)(43) + \tau_2(\dots\text{OHH}\dots)(45) + \gamma(\dots\text{HHO}\dots)(13)$
b		604	3	+7		$\delta_{\text{R}3}(41) + \delta(\text{C}_2\text{O})(11) + \nu(\text{C}_6\text{N}_1)(11) + \delta(\text{C}_4\text{N})(12) + \delta(\text{N}_1\text{C}_{10})(13)$
572?	+8?	558	15	+4		$\delta(\text{C}_2\text{O})(33) + \delta_{\text{R}3}(27)$
b		466	8	+3		$\delta_{\text{R}2}(64) + \nu(\text{N}_1\text{C}_{10})(11)$
423	+8	410	21	+7		$\tau_{\text{R}2}(62) + \tau_{\text{R}1}(27) + \gamma(\text{C}_4\text{N})(12)$
c		359	71	+2		$\delta(\text{C}_4\text{N})(27) + \delta(\text{C}_2=\text{O})(14) + \tau_1(\dots\text{OHH}\dots)(31)$
c		323	36	+3		$\delta(\text{N}_1\text{C}_{10})(64) + \delta(\text{C}_4\text{N})(27)$
c		266	155	+132		$\text{wag}(\text{NH}_2)(58) + \tau(\text{NH}_2)(22) + \gamma(\dots\text{HHO}\dots)(16)$
c		237	5	+5		$\gamma(\text{N}_1\text{C}_{10})(63) + \tau_{\text{R}1}(17)$
c		179	1	-1		$\tau_{\text{R}2}(34) + \tau_{\text{R}1}(26) + \gamma(\text{N}_1\text{C}_{10})(20)$
c		108	0.2	+4		$\tau(\text{CH}_3)(68) + \gamma(\text{N}_1\text{C}_{10})(29)$
c		101	4	+3		$\tau_{\text{R}3}(82) + \tau(\text{CH}_3)(21)$

^a Water modes unscaled, base modes uniformly scaled with 0.90. ^b Too weak to be observed. ^c Situated below studied region. ^d See Table 2; description of intermolecular modes as in 4-NH₂-pyrimidine·H₂O.²

bands in this region, while the shifted $\tau(\text{NH}_2)$ (coupled to intermolecular modes in this case) is predicted to be very weak. Furthermore, the shift of the $\nu^a(\text{NH}_2)$ mode cannot be used to discriminate between the two N₃...H-O...H-N₁₄ and N₁₄-H...OH₂ complex species because comparable shifts are predicted in both cases (Tables 8 and 9). Although a noticeably smaller shift is predicted for the $\nu^s(\text{NH}_2)$ mode in the open complex, the predicted shift is not far from the experimental shift for the abundant, closed complex and both may overlap. The only indication for the presence of the open N₁₄-H...OH₂ complex is then the shift of the water ν_3 mode. As a matter of fact, a clear broadening of the dimer acceptor band is observed

at 3722 cm⁻¹ (Figure 2), and this feature is tentatively assigned to the open N₁₄-H...OH₂ complex structure.

Another complex species of a-o IMC, which is undoubtedly present in the low-temperature Ar matrix, is the open C₂=O...H-OH structure. Although no comparison can be made with *ab initio* predicted spectral parameters for this complex because it is not predicted to be stable by the calculations at the SCF/6-31++G** level (Table 6), some of the spectral perturbations induced by water in the experimental spectra are very similar to those observed for open complexes involving H-bonded water at the carbonyl group of uracils,³⁵ MOP, and TMC.⁴ This is demonstrated in Table 10, which

TABLE 9: Summary of Calculated Spectral Parameters for H-Bond Sensitive Modes in Different H-Bonded Complexes of Water with the Amino-Oxo Tautomer of 1-CH₃-Cytosine

complex mode ^b	N ₃ ...H-OH...O ₇ ^a			N ₁₄ -H...OH ₂			N ₁₄ ...H-OH		
	ν (cm ⁻¹)	I (km/mol)	shift (cm ⁻¹)	ν (cm ⁻¹)	I (km/mol)	shift (cm ⁻¹)	ν (cm ⁻¹)	I (km/mol)	shift (cm ⁻¹)
$\nu_{\text{OH}}^{\text{f}}$	4218	97	-49	4257	120	-10	4243	180	-24
$\nu_{\text{OH}}^{\text{b}}$	4119	205	-27	4140	42	-6	4112	10	-34
$\nu^{\text{a}}(\text{NH}_2)$	3599	77	+7	3571	163	-21	3536	56	-58
$\nu^{\text{s}}(\text{NH}_2)$	3469	123	+5	3438	258	-25	3422	71	-41
$\nu(\text{C}=\text{O})$	1751	675	+22	1721	902	-8	1733	913	+4
$\delta(\text{HOH})$	1820	223	+90	1745	163	+15	1745	58	+15
$\nu(\text{C}_4\text{N})^{\text{c}}$	1370	352	+12	1360	394	+2	1355	353	-3
$\tau(\text{NH}_2)$	540	102	+25	612	5	+97	496	39	-18

^a Spectral parameters calculated at the SCF/6-31G** level for this complex. ^b Water modes unscaled, base modes uniformly scaled with 0.90. ^c Mode with large PED contribution of this bond stretch.

TABLE 10: Spectral Characteristics of the C₂=O...H-OH Complex in 4-Thiouracil (4SU), 1-CH₃-2-Pyrimidone (MOP), 1-Methylcytosine (IMC), and N,N-1-TriCH₃-Cytosine (TMC)

mode or shift (cm ⁻¹)	4SU ³⁵	MOP ⁴	IMC	TMC ⁴
$\nu_{\text{OH}}^{\text{b}}$	3524	3493/3487	3469	3465
$\nu_{\text{OH}}^{\text{f}}$	3706	3705	3704	3703
$\Delta\nu(\text{C}=\text{O})$	-18	-17	-18	-21

summarizes these vibrational characteristics for different, open C₂=O...H-OH species identified in Ar matrices. The most important spectral manifestations of this complex species are the shifts of the $\nu(\text{C}=\text{O})$ and $\gamma(\text{C}=\text{O})$ modes. Observation of the $\nu_{\text{OH}}^{\text{f}}$ and $\nu_{\text{OH}}^{\text{b}}$ bands at 3704 and 3469 cm⁻¹ is also consistent with the open C₂=O...H-OH structure. The intensity of the $\nu_{\text{OH}}^{\text{b}}$ band at 3469 cm⁻¹ is noticeably smaller than that of the other $\nu_{\text{OH}}^{\text{b}}$ band for the N₃...H-O...H-N₁₄ complex (3350 cm⁻¹), which indicates a substantially larger abundance of the latter species, in accordance with its great stability (Table 6). Since H-bonding at the proton-acceptor sites in the ring of amino-pyrimidines and amino-pyridines causes only small frequency increases of the amino stretches,² the weak features observed at the high-frequency side of the monomer $\nu^{\text{a}}(\text{NH}_2)$ and $\nu^{\text{s}}(\text{NH}_2)$ in Figure 2 are considered to be further manifestations for the presence of the C₂=O...H-OH species. The discrepancy between the experimental observation (open complex) and the predicted interaction (anticooperatively closed complex) is extensively discussed in our paper on MOP and TMC.⁴

Due to the small amount of the imino-oxo *E* tautomer of IMC present in the matrix, the experimental search for water complexes of this tautomer is more difficult. Only complex absorptions related to very intense modes of the *i*-o *E* form (Table 4) can be used for this purpose and probably only for samples with a large amount of water. Furthermore, only absorptions of the most stable complex N₁₄...H-O...H-N₃ predicted for this tautomer will be observable. Figure 4 illustrates some experimentally observed perturbations of the *i*-o *E* bands at high water content or after repeated annealing of the matrix: a shifted $\nu(\text{N}_3\text{H})$ mode at 3290 (-140)⁴³ cm⁻¹, the perturbed $\nu(\text{C}=\text{O})$ mode at 1737 (+6) cm⁻¹, and the frequency-decreased $\nu(\text{C}_4=\text{N}_{14})$ mode at 1664 (-10) cm⁻¹. These shifts agree rather well with the *ab initio* predicted shifts for the cooperative, closed N₁₄...H-O...H-N₃ complex of the *i*-o *E* tautomer as is shown in Table 11 summarizing the predicted perturbations for the sensitive modes of the three complexes of this tautomeric form. An experimental shift (-140 cm⁻¹) larger than the theoretically predicted shift (-95 cm⁻¹, optimal scaling factor of 0.875) for the bonded N-H... stretch probably originates from the increased anharmonicity of this vibration due to the H-bonding, and comparable results have been found for 2-pyridone·H₂O ($\Delta\nu_{\text{N-H...}} = -168$ cm⁻¹

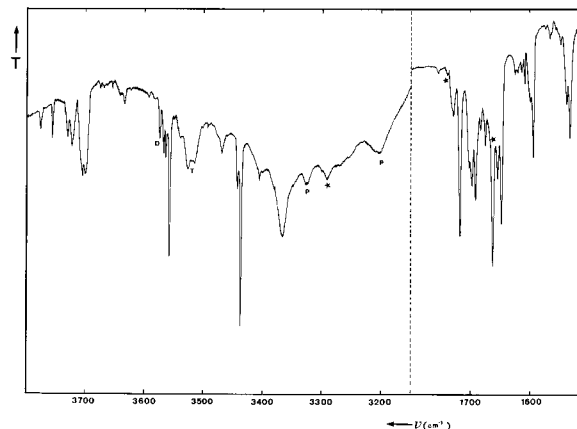


Figure 4. High-frequency (left) and the $\nu(\text{C}=\text{O})$ (right) region of the FT-IR spectrum of 1-CH₃-cytosine/H₂O/Ar (H₂O/Ar = 1/100) at 12 K (★ = N₁₄...H-O...H-N₃ complex of rare *i*-o *E* tautomer; D, T, P are defined as in Figure 2).

from experiment vs -76 cm⁻¹ from theory, optimal scaling factor of 0.865).³⁶ The $\nu_{\text{OH}}^{\text{f}}$ mode for the closed complex of *i*-o *E* IMC is predicted to be at nearly the same frequency and the $\nu_{\text{OH}}^{\text{b}}$ mode at exactly the same frequency as that for the N₃...H-O...HN₁₄ complex of the abundant *a*-o tautomer, so these characteristic bands cannot be used to demonstrate the presence of the closed complex of the *i*-o *E* form. However, the shifts of the internal base modes mentioned above are strong indications for the presence of a small amount of the most stable N₁₄...H-O...H-N₃ complex of the *i*-o *E* tautomer of IMC, and this is the first experimental observation of a H-bonded structure of this rare tautomer in the IR spectrum.

Correlation Between $\Delta\nu_{\text{OH}}^{\text{b}}$ and $\text{PA}_{\text{C}=\text{O}}$ for Open C=O...H-OH Complexes. We have demonstrated formerly that the experimental frequency shift of H-bonded water can be used to estimate the proton affinity (PA) of the basic atom involved in the H-bond interaction. A correlation curve relating these two parameters was developed for open N...H-OH complexes of a series of the pyridine/pyrimidine type bases.^{2,3,37} This correlation has been used to estimate PA_{N} values of 4-NH₂-pyrimidine, 3-OH-pyridine, and 4-OH-pyridine with a good accuracy.³

The identification of the open C=O...H-OH complexes in the FT-IR spectra of MOP·H₂O and TMC·H₂O⁴ as well as of IMC·H₂O in this work allows us to establish the same type of correlation for C=O...H-OH complexes. Contrary to our earlier attempts to correlate large sets of data for different types of O and S bases in different matrices as well as in solution,³⁸ here we would like to find the correlation for only C=O...H-OH complexes examined in Ar matrices for which PA values are exactly known or accurately estimated. Figure 5 illustrates the correlation obtained for the complexes of water with formal-

TABLE 11: Summary of Calculated Spectral Parameters for H-Bond Sensitive Modes in Different H-Bonded Complexes of Water with the Imino-Oxo *E* Tautomer of 1-CH₃-Cytosine

complex mode ^a	N ₁₄ ...H-O...H-N ₃			O ₇ ...H-O...H-N ₃			N ₁₄ ...OH ₂		
	ν (cm ⁻¹)	<i>I</i> (km/mol)	shift ^c (cm ⁻¹)	ν (cm ⁻¹)	<i>I</i> (km/mol)	shift (cm ⁻¹)	ν (cm ⁻¹)	<i>I</i> (km/mol)	shift (cm ⁻¹)
ν_{OH}^f	4233	142	-34	4243	151	-24	4258	107	-9
ν_{OH}^b	3997	325	-149	4070	147	-96	4141	41	-5
$\nu(N_3H)$	3382	227	-95 (-140)	3392	16	-85	3480	81	+3
$\nu(N_{14}H)$	3418	21	+7	3409	232	-2	3414	91	+3
$\nu(C=O)$	1752	927	+6 (+6)	1723	1173	-23	1739	967	-7
$\nu(C=N_{14})^b$	1691	927	-14 (-10)	1709	548	+4	1709	863	+4
$\delta(HOH)$	1756	203	+26	1739	225	+9	1742	133	+12
$\gamma(C=O)^b$	772	87	0	776	48	+4	760	82	-12

^{a,b} See Table 9 footnotes b and c. ^c Experimental value in parentheses.

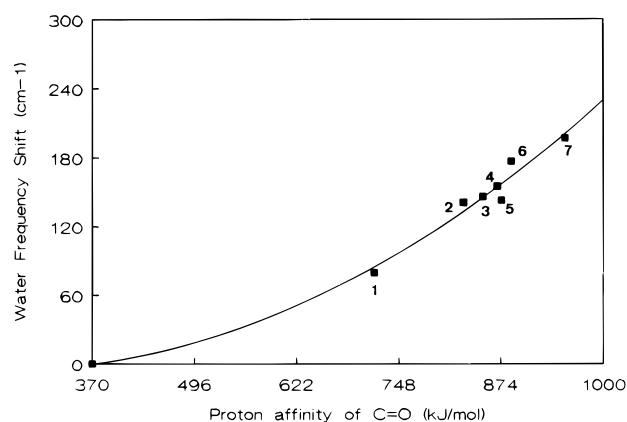


Figure 5. Correlation between the corrected frequency shift $\Delta\nu_{OH}^b$ of the bonded water mode and the proton affinity value of the C=O group in C=O...HO-H complexes: 1 = formaldehyde; 2 = methyl acetate; 3 = methyl benzoate; 4 = uracil; 5 = 2-thiouracil; 6 = 1-CH₃-2-pyrimidone; 7 = *N,N*-1-triCH₃-cytosine.

dehyde, methyl acetate, methyl benzoate, 2-thiouracil, uracil (all data taken from ref 38), MOP, and TMC. The point (370:0) at the origin has been based on the PA value of Ar.³⁹ The correlation is not as regular as that for open N...H-OH systems shown further, and additional systems must be added in the future to more firmly establish the correlation trend. The preliminary, best mathematical representation for the curve in Figure 5 is the polynomial

$$\Delta\nu_{OH}^b = 21.84 - 0.218PA + 0.00043(PA)^2 \quad (r = 0.991)$$

Insertion of the $\Delta\nu_{OH}^b$ value for the open C=O...H-OH complex of a-o 1MC into the correlation suggests that the $PA_{C=O}$ value of the a-o tautomer of 1MC is close to the value of 953 kJ/mol for TMC, which has been estimated from an accurate correlation based on H-bonded complexes with phenol in solution.⁴ This is what can be expected, since the N₁ atom is substituted by a CH₃ group in both compounds, whereas further substitution on the amino group in TMC should affect only the $PA(N_3)$ value.

H-Bond Cooperativity in Closed N...H-O...H-N Complexes. The concept of H-bond cooperativity implies that formation of a second H-bond with HA', H-A...H-A', on the proton-acceptor site of the molecule whose H-A group is already involved in a H-bond with B, B...H-A, strengthens the latter H-bond.⁴⁰ The degree of mutual H-bond fortification can be obtained by considering the ratio of the frequency shifts, $\Delta\nu_{HA}$, of the complexes B...H-A...H-A' and B...H-A, respectively.⁴¹ These so-called "cooperativity factors" have been quantitatively investigated using matrix spectral data for the open 1:2 complexes B'...H-A...H-A involving the proton donors HF, HCl, and HOH.⁴² Contrary to these linear 1:2 complexes, the optimal geometry for the 2-fold intermolecular interaction

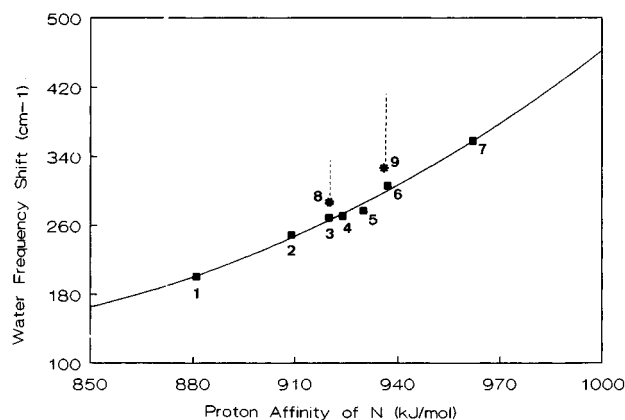


Figure 6. Correlation between the corrected frequency shift $\Delta\nu_{OH}^b$ of the bonded water mode and the proton affinity value of the N atom in open N...HO-H complexes: 1 = pyrimidine; 2 = 4-NH₂-pyrimidine (N₁); 3 = 3-OH-pyridine; 4 = pyridine; 5 = imidazole; 6 = 4-OH-pyridine; 7 = 4-NH₂-pyridine; 8 = 4-NH₂-pyrimidine N₃...H-O...H-N; 9 = 1-CH₃-cytosine N₃...H-O...H-N.

is not always possible in the case of the closed complex with two H-bonds such as the most stable a-o 1MC complex found in this work. In this type of "pseudo" 1:2 complex, the mutual H-bond fortification will be opposed by a necessary distortion of the geometry for both H-bonds because of spatial constraints of B, the latter being a single molecule with two H-bonding sites in this case, and therefore, smaller cooperativity factors than for linear 1:2 complexes are expected. Nevertheless, the frequency shift of the doubly bonded water molecule in the closed complex will still be larger than expected from the PA value of the most basic center, which is the N₃ atom in the case of the N₃...H-O...H-NH complexes.

This phenomenon can be illustrated using the correlation $\Delta\nu_{OH}^b = f(PA_N)$ for open N...HO-H complexes mentioned above (Figure 6). Assuming that the PA_N value for the N₃ atom in 1MC is about equal to that of the similar site in cytosine—the latter value being known from experiment³⁹—insertion of the experimental $\Delta\nu_{OH}^b$ value found in this work (Table 8) yields a point situated above the correlation curve. The larger than expected frequency shift from the $PA(N_3)$ value originates from cooperativity between the two H-bonds in the closed complex. The same observation is made for the closed complex observed earlier for 4APM·H₂O, for which a $PA(N_3)$ value of about 920 kJ/mol can be estimated.^{2,44} If the H-bond cooperativity was as large as in linear B...H-O...H-O complexes (cooperativity factor of 1.37),⁴² the deviation from the correlation would be much larger, as indicated by the dotted lines in Figure 6.

Summary

The combined matrix-isolation FT-IR and theoretical *ab initio* 6-31++G** method has been applied to investigate the 1-CH₃-

cytosine tautomerism and H-bonding with water. The *ab initio* assisted analysis of the IR spectrum of 1-CH₃-cytosine in Ar indicates the presence of trace amounts of the rare imino-oxo *E* form of the base. A combination of the experimental and theoretical predicted IR intensities of some characteristic bands of the amino-oxo and imino-oxo *E* tautomers allows us to estimate a tautomerization constant $K_T(a-o/i-o E)$ value of 7.2. Among the four predicted stable H-bonded complexes of the abundant *a-o* tautomer with water, the most stable one is the closed N₃...H-O...H-N₁₄ structure, and this complex is identified in the experimental spectrum. A rather weak cooperativity between the two H-bonds exists in this closed structure. Evidence is obtained for the presence of an additional, open C₂=O...H-OH complex. Relevant spectral data for this complex are correlated with the data of similar compounds involving carbonyl-water H-bonds. H-bonding of the rare imino-oxo *E* IMC tautomer with water is experimentally detected for the first time. The spectral data suggest a closed N₁₄...H-O...H-N₃ structure for this interaction in accordance with the *ab initio* energetic and spectral predictions.

Acknowledgment. This work was supported by the NATO International Collaborative Grant INT-9313268. L. Adamowicz acknowledges the Office of Health and Environmental Research, Office of Energy Research, Department of Energy (Grant No. DEFG 0393ER61605) for supporting the postdoctoral research of J. Smets at the University of Arizona. L. Adamowicz also acknowledges support of his stay at the Paul Sabatier University (Toulouse, France) from the CNRS of France. L. Adamowicz thanks Professors J.-P. Daudey and J.-P. Mathieu for their hospitality. G. Maes is grateful to the Belgian NFWO for a permanent research fellowship. The authors also acknowledge Dr. L. Lapinski (Institute of Physics, Polish Academy of Sciences, Warsaw, Poland) for the use of the PED calculation program.

Supporting Information Available: Table listing *ab initio* geometry parameters of amino-oxo 1-CH₃-cytosine, imino-oxo *E* 1-CH₃-cytosine, and H-bonded complexes with water (2 pages). Ordering information is given on any current masthead page.

References and Notes

- (1) Destexhe, A.; Smets, J.; Adamowicz, L.; Maes, G. *J. Phys. Chem.* **1994**, *98*, 1506.
- (2) Smets, J.; Adamowicz, L.; Maes, G. *J. Phys. Chem.* **1995**, *99*, 6387.
- (3) Buyl, F.; Smets, J.; Maes, G.; Adamowicz, L. *J. Phys. Chem.* **1995**, *99*, 14967.
- (4) Destexhe, A.; Smets, J.; Adamowicz, L.; Maes, G. To be published.
- (5) Szczesniak, M.; Kwiatkowski, J. S.; KuBulat, K.; Szczepaniak, K.; Person, W. B. *J. Am. Chem. Soc.* **1988**, *110*, 8319.
- (6) Lapinski, L.; Nowak, M. J.; Fulara, J.; Les, A.; Adamowicz, L. *J. Phys. Chem.* **1990**, *94*, 6555.
- (7) Smets, J.; Adamowicz, L.; Maes, G. To be published.
- (8) Saenger, W. *Principles of Nucleic Acid Structure*; Springer: New York, 1984.
- (9) Fazakerly, G. V.; Gdaniec, Z.; Sowers, L. C. *J. Mol. Biol.* **1993**, *230*, 10.
- (10) Szczesniak, M.; Leszczynski, J.; Person, W. B. *J. Am. Chem. Soc.* **1992**, *114*, 2731.
- (11) Pullman, A.; Perahia, D. *Theor. Chim. Acta* **1978**, *48*, 29.
- (12) Del Bene, J. E. *J. Comput. Chem.* **1983**, *4*, 226.
- (13) De Oliveria-Neto, M. *J. Comput. Chem.* **1986**, *7*, 617.
- (14) Berman, H. M.; Sowri, A.; Ginell, S.; Beveridge, D. J. *Biomol. Struct. Dyn.* **1988**, *5*, 1101.
- (15) Sagarik, K.; Corongiu, G.; Clementi, E. *J. Mol. Struct.: THEOCHEM* **1991**, *235*, 355.
- (16) Maes, G. *Bull. Soc. Chim. Belg.* **1981**, *90*, 1093.
- (17) Graindourze, M.; Smets, J.; Zeegers-Huyskens, Th.; Maes, G. *J. Mol. Struct.* **1990**, *222*, 345.
- (18) Frisch, C. M.; Trucks, G. W.; Head-Gordon, M.; Gill, P. M. W.; Wong, W. M.; Foresman, J. B.; Johnson, B. G.; Schlegel, H. B.; Robb, M. A.; Replogie, E. S.; Gomperts, R.; Andres, J. L.; Raghavachari, K.; Binkley, J. S.; Gonzales, C.; Martin, R. L.; Fox, D. J.; Defrees, D. J.; Baker, J.; Stewart, J. J. P.; Pople, J. A. *GAUSSIAN 92*; Gaussian Inc.: Pittsburgh, PA, 1992.
- (19) Katritzky, R. K.; Karelson, M. *J. Am. Chem. Soc.* **1991**, *113*, 1561.
- (20) Les, A.; Kukawska-Tarnawska, B. *J. Mol. Struct.: THEOCHEM* **1986**, *148*, 45.
- (21) Person, W. B.; Szczepaniak, K.; Szczesniak, M.; Kwiatkowski, J. S.; Hernandez, L.; Czerminski, R. *J. Mol. Struct.* **1989**, *194*, 239.
- (22) Szczesniak, M.; Nowak, M. J.; Szczepaniak, K. *J. Mol. Struct.* **1984**, *115*, 221.
- (23) Radchenko, Ye. D.; Plokhotnichenko, A. M.; Sheina, G. G.; Blagoi, Yu. P. *Biofizika* **1983**, *4*, 592.
- (24) Person, W. B.; Szczepaniak, K. In *Vibrational Spectra and Structure*; Durig, J. R., Ed.; Elsevier: Amsterdam, 1993; Vol. 20, pp 239–325.
- (25) Nowak, M. J.; Lapinski, L.; Fulara, J.; Les, A.; Adamowicz, L. *J. Phys. Chem.* **1991**, *95*, 2404.
- (26) Smets, J.; Maes, G. *Chem. Phys. Lett.* **1991**, *187*, 532.
- (27) Vranken, H.; Smets, J.; Maes, G.; Lapinski, L.; Nowak, M. J.; Adamowicz, L. *Spectrochim. Acta Part A* **1994**, *50*, 875.
- (28) Kwiatkowski, J. S.; Leszczynski, J. *Chem. Phys. Lett.* **1993**, *204*, 430.
- (29) Moreno, M.; Miller, W. H. *Chem. Phys. Lett.* **1990**, *171*, 475.
- (30) Field, M. J.; Hillier, I. H. *J. Chem. Soc., Perkin Trans. 2* **1987**, *2*, 617.
- (31) Fabian, W. M. F. *J. Phys. Org. Chem.* **1990**, *3*, 332.
- (32) Les, A.; Adamowicz, L.; Nowak, M. J.; Lapinski, L. *J. Mol. Struct.: THEOCHEM* **1994**, *312*, 157.
- (33) Kulawkowski, I.; Geller, M.; Lesyng, B.; Bolewska, K.; Wierzchowski, K. L. *Biochim. Biophys. Acta* **1975**, *407*, 420.
- (34) Engdahl, A.; Nelander, B. *J. Mol. Struct.* **1989**, *193*, 101.
- (35) Graindourze, M.; Grootaers, T.; Smets, J.; Zeegers-Huyskens, Th.; Maes, G. *J. Mol. Struct.* **1991**, *243*, 37.
- (36) Smets, J. Ph.D. Thesis, University of Leuven, Heverlee, Belgium, 1993.
- (37) Van Bael, M. K.; Schoone, K.; Smets, J.; McCarthy, W.; Adamowicz, L.; Nowak, M. J.; Maes, G. In preparation.
- (38) Maes, G.; Smets, J. *J. Mol. Struct.* **1992**, *270*, 141.
- (39) Lias, S. G.; Liebman, J. F.; Levin, R. D. *J. Phys. Chem. Ref. Data* **1984**, *13*, 695.
- (40) Frank, H. S.; Wen, W.-Y. *Discuss. Faraday Soc.* **1957**, *24*, 133.
- (41) Kleeberg, H. In *Intermolecular Forces. An Introduction to Modern Methods and Results*; Huyskens, P., Luck, W. A. P., Zeegers-Huyskens, Th., Eds.; Springer-Verlag: Berlin, 1991; pp 195–216.
- (42) Maes, G.; Smets, J. *J. Phys. Chem.* **1993**, *97*, 1825.
- (43) This shift was calculated using the value for the free $\nu(N_3H)$ mode taken from ref 10.
- (44) This value is obtained by adding the difference between PA(N₁) values for 4-NH₂-pyridine and pyridine to the PA(N₃) value of pyrimidine.

JP951167V